

Clinical characteristics and management of retinitis pigmentosa

Nguven, X.T.

Citation

Nguyen, X. T. (2024, January 23). *Clinical characteristics and management of retinitis pigmentosa*. Retrieved from https://hdl.handle.net/1887/3714325

Version: Not Applicable (or Unknown)

Licence agreement concerning inclusion of doctoral

License: thesis in the Institutional Repository of the University

of Leiden

Downloaded from: https://hdl.handle.net/1887/3714325

Note: To cite this publication please use the final published version (if applicable).



CHAPTER 2.4

CRB1-ASSOCIATED RETINAL DYSTROPHIES: A PROSPECTIVE NATURAL HISTORY STUDY IN ANTICIPATION OF FUTURE CLINICAL TRIALS

Xuan-Thanh-An Nguyen¹, Mays Talib¹, Mary J. van Schooneveld², Jan Wijnholds¹, Maria M. van Genderen^{4,5}, Nicoline E. Schalij-Delfos¹, Caroline C.W. Klaver^{6,7,8,9}, Herman E. Talsma^{1,4}, Marta Fiocco^{10,11}, Ralph J. Florijn¹², Jacoline B. ten Brink¹², Frans P.M. Cremers¹³, Magda A. Meester-Smoor⁶, L. Ingeborgh van den Born¹⁴, Carel B. Hoyng⁸, Alberta A.H.J. Thiadens⁶, Arthur A. Bergen^{3,12}, and Camiel J.F. Boon^{1,2}

Am J Ophthalmol 2021; 234: 37-48



¹ Department of Ophthalmology, Leiden University Medical Center, Leiden, the Netherlands.

² Department of Ophthalmology, Amsterdam UMC, Academic Medical Center, Amsterdam, the Netherlands.

³ The Netherlands Institute for Neuroscience (NIN-KNAW), Amsterdam, The Netherlands.

⁴ Bartiméus, Diagnostic Centre for complex visual disorders, Zeist, the Netherlands.

⁵ Department of Ophthalmology, University Medical Centre Utrecht, Utrecht, the Netherlands.

⁶ Department of Ophthalmology, Erasmus Medical Center, Rotterdam, the Netherlands.

⁷ Department of Epidemiology, Erasmus University Medical Center, Rotterdam, The Netherlands.

⁸ Department of Ophthalmology, Radboud University Medical Center, Nijmegen, the Netherlands.

⁹Institute for Molecular and Clinical Ophthalmology, Basel, Switzerland.

¹⁰ Mathematical Institute Leiden University, Leiden, The Netherlands.

¹¹ Department of Biomedical Data Sciences, Leiden University Medical Center, Leiden, The Netherlands.

¹² Department of Clinical Genetics, Amsterdam UMC, Academic Medical Center, Amsterdam, the Netherlands.

¹³ Department of Human Genetics and Donders Institute for Brain, Cognition and Behaviour, Radboud University Medical Center, Nijmegen, the Netherlands.

¹⁴ Rotterdam Eye Hospital, Rotterdam, the Netherlands.

ARSTRACT

Purpose

To describe the natural disease course of *CRB1*-associated retinal dystrophies, and to identify clinical endpoints for future clinical trials.

Design

Single center, prospective cohort study.

Methods

An investigator-initiated nationwide collaborative study that included 22 patients with *CRB1*-associated retinal dystrophies. Patients underwent ophthalmic assessment at baseline and 2 years after baseline. Clinical examination included best-corrected visual acuity (BCVA) using ETDRS charts, Goldmann kinetic perimetry (V4e isopter seeing retinal areas), microperimetry, full-field electroretinography (ERG), full-field stimulus threshold (FST), fundus photography, spectral-domain optical coherence tomography and fundus autofluorescence imaging.

Results

Based on genetic, clinical and electrophysiological data, patients were diagnosed with retinitis pigmentosa (n = 19; 86%), cone-rod dystrophy (n = 2; 9%) or isolated macular dystrophy (n = 1; 5%). Two-year analysis of the entire cohort showed no significant changes in BCVA (p = 0.069) or V4e isopter seeing retinal areas (p = 0.616), although signs of clinical progression were present in individual patients. Macular sensitivity measured on microperimetry revealed a significant reduction at 2-year follow-up (p < 0.001). FST responses were measurable in patients with non-recordable ERGs. On average, FST responses remained stable during follow-up.

Conclusion

In *CRB1*-associated retinal dystrophies, visual acuity and visual field measures remain relatively stable over the course of 2 years. Microperimetry showed a significant decrease in retinal sensitivity during follow-up, and may be a more sensitive progression marker. Retinal sensitivity on microperimetry may serve as a functional clinical endpoint in future human treatment trials for *CRB1*-associated retinal dystrophies.

INTRODUCTION

A wide range of related retinal dystrophies (RDs), including Leber congenital amaurosis (LCA), retinitis pigmentosa (RP) and cone(-rod) dystrophies, can be caused by variants in the *CRB1* gene.¹⁻⁴ LCA is considered the most severe retinal dystrophy, presenting at birth or early infancy, and is characterized by severe visual impairment, nystagmus, poor pupillary responses, and absent responses on electroretinography.⁴ RP is characterized by primary degeneration of rod photoreceptors, with secondary cone degeneration. Initial symptoms in RP typically include night blindness due to degeneration of the rods, followed by concentric visual field loss, and eventually central vision loss later in life due to cone dysfunction.⁵ RP comprises a broad spectrum of phenotypic presentations, and can become symptomatic at different ages, ranging from early childhood (i.e. juvenile RP) to middle age, caused by a broad spectrum of genes.⁶

The *CRB1* gene encodes the transmembrane protein Crumbs homologue 1 (CRB1) which, in mammals, localizes to the subapical region of Müller and photoreceptor cells. ⁷⁻¹⁰ The canonical isoform of CRB1 consists of 19 epidermal growth factor domains and 3 laminin A globular-like domains, and a short cytoplasmic tail that contains FERM/PDZ binding motifs. ¹¹ Recently, a novel isoform of CRB1, CRB1-B, was also discovered, which is presumed to be more abundant in the human retina than its canonical form. ¹² While the function of CRB1 in the human retina has not been fully elucidated, it has been suggested to play a key role in cell polarity, cell-to-cell adhesion, photoreceptor morphogenesis and retinal maturation. ^{8,13-16} The role of CRB1 in retinal development is supported by the abnormal thickening and coarse lamination of the inner retinal layers that has been described in the majority of cases of *CRB1*-associated RDs, which strikes a resemblance to an immature retina. ¹⁷ Other clinical features described in *CRB1*-associated RDs include hyperopia, optic nerve drusen, preservation of para-arteriolar retinal pigment epithelium, cystoid macular edema, nummular pigmentation and Coats-like exudates. ¹⁸

Currently, no treatment exists for patients with *CRB1*-associated RDs, but proof-of-concept of adeno-associated virus-mediated gene transfer was achieved using murine models. ^{15,19} As *CRB1* gene therapy is being developed, it is crucial to determine adequate clinical endpoints ahead of these upcoming trials. ¹⁰ This requires an optimal understanding of the disease; its variability and its progression, based on retrospective and prospective natural history studies. ²⁰ A retrospective study previously performed by our study group provided insights into the progressive decline in visual acuity and visual fields in patients with *CRB1* variants, showing that the optimal window for treatment is likely within the first 2 to 3 decades of life based on these outcome measures. ¹⁸ However, our knowledge on the feasibility of other psychophysical

outcome measures, such as microperimetry and full-field-stimulus thresholds, remains limited 18,21

Herein, we report the first prospective natural history study performed in 22 patients with biallelic *CRB1* variants. The objective of this study was to describe the disease progression in *CRB1*-associated retinal dystrophies, and to determine potential clinical endpoints in anticipation of future therapeutic trials. Based on these findings, we provide the first recommendations and considerations for the study design of upcoming *CRB1* clinical trials.

METHODS

Patient recruitment

This nationwide collaborative study recruited patients from 2 different registries: the RD5000 database, which is a national registry for inherited retinal diseases; and the Delleman archive for genetic eye diseases at Amsterdam University Medical Center. Inclusion criteria for this study were the presence of biallelic *CRB1* variants with a RD phenotype, and a best-corrected visual acuity (BCVA) of \geq 20/400 Snellen acuity. In total, 22 patients with biallelic *CRB1* variants were included in the study, of which 10 patients (45%) originated from a previously described genetically isolated population. Patients were examined at baseline and 2 years after baseline at Leiden University Medical Center.

The study protocol, genetic findings, and baseline characteristics of the included patients have been described in detail elsewhere, and are briefly described herein.²⁴ The current study presents the 2-year follow-up data, and describes the longitudinal findings in this cohort.

The study protocol was approved by the Medical Ethics Committee of the Erasmus Medical Center, as it was performed within the framework of the RD5000, and from the local review board of Leiden University Medical Center. Informed consent was obtained from individuals and/or legal guardians, and the study adhered to the tenets of the Declaration of Helsinki

Clinical examination

Refraction and BCVA were measured monocularly, using the Early Treatment Diabetic Retinopathy Study (ETDRS) letter chart. ETDRS letters were converted to Logarithm of the Minimum Angle of Resolution (logMAR) values for statistical analysis. Visual fields (V4e isopter) were obtained using Goldmann perimetry, which were subsequently converted to digital seeing retinal areas (in mm²) using a method described by Dagnelie.² A change ≥20% in retinal seeing area was considered clinically significant

based on previous test-retest reliability studies in RP patients.²⁶ Macular sensitivity was assessed by MAIA microperimetry (Centervue, Padova, Italy) using the standard 37-stimuli grid pattern under mesopic conditions. Fixation stability was quantified using the 95% bivariate contour ellipsoid areas (BCEA), which encompasses 95% of all the fixation points during examination. To minimize a learning effect, subjects first underwent a practice session (fixed strategy), prior to formal testing using the 4-2 threshold strategy.^{27,28} For follow-up measurements, the inbuilt follow-up software of the MAIA microperimetry was used, enabling accurate reassessment of the same test loci evaluated at baseline. If automatic alignment failed, manual alignment was performed using characteristic retinal landmarks.

After 30 minutes of dark-adaption, full-field electroretinography (ERG) responses were recorded on the Diagnosys (Cambridge, UK) using Dawson Trick Litzkow electrodes, which incorporated the International Society for Clinical Electrophysiology Standards (ISCEV). ERGs were only repeated at follow-up in patients with residual ERG function. Full-field stimulus threshold (FST; Diagnosys LLC, Lowell, MA, USA) testing was performed in a subset of patients using white and chromatic stimuli with the reference luminance (0 dB) set to 0.01 cds/m² (25 cd/m² presented for 4 ms). Based on FST data by previous studies, the normal threshold for white stimuli, while accounting for differences in reference luminance, should be set at -53 dB.²⁹⁻³¹ Thresholds were measured in triplicate for each stimulus and were averaged per eye. Differences between averaged chromatic sensitivities were used to determine whether responses were rod-mediated (blue-red difference of >22 dB), cone-mediated (blue-red difference of <3 dB), or mixed rod-and-cone-mediated (blue-red difference between 3-22 dB).^{29.32}

Retinal imaging included fundus photography (Topcon TRC-50DX, Topcon Medical Systems, Inc. Oakland, NJ, USA), spectral-domain coherence tomography (SD-OCT; Spectralis, Heidelberg Engineering, Germany), and 488 nm wavelength fundus autofluorescence (FAF; Heidelberg Engineering, Germany). On SD-OCT, the laminar organization of the inner retinal layers (inner limiting membrane through external limiting membrane) was categorized into 3 different grades: [1] normal organization without coarse lamination; [2] normal organization with coarse lamination; and [3] relative disorganization with coarse lamination. In addition, the integrity of two hyperreflective bands of the outer retina were evaluated at the (para)fovea (within 2.5 mm of the foveal center) and perifovea (outside 2.5 mm of the foveal center): the external limiting membrane (ELM), and the ellipsoid zone (EZ). The retinal bands were either defined as: continuous, discontinuous or indiscernible. Overall definitions and example gradings of the inner and outer retina are provided in Supplementary Figure 1. SD-OCT images were assessed by two authors (XN and MT) and reviewed by CJFB in case of discrepancy between the aforementioned two authors.

Statistical Analysis

Data analysis was performed using R version 3.6.2 (R Foundation for Statistical Computing, Vienna, Austria). The normality of data was analyzed using the Shapiro-Wilk test, and was also visually plotted. Continuous data were either presented as mean, standard deviations (SD), and range, in the case of normal distribution; and as median, interquartile ranges (IQR), and range, in the case of non-normal distribution. Categorical data were presented as frequencies and percentages. Changes in parameters between baseline and follow-up were assessed using a linear mixed effect model while accounting for paired eye data within patients. Correlation testing was performed using Spearman's correlation test, using data of the right eye only. The level of significance was set at 0.05. Bonferroni adjustments were applied for multiple testing where appropriate.

RESULTS

Clinical and genetic characteristics

Twenty-two patients, of which 10 (45%) originated from a previously described genetically isolated population, were assessed at baseline and at 2-year follow-up. 24 A summary of the clinical findings in this cohort is provided in Table 1, and is also described for each individual patient in Supplemental Table S1. Patients had a median age of 25.7 years (IQR 19.4; range 6.2 - 74.8) at baseline, and a mean follow-up time of 2.04 years (SD \pm 0.05; range 1.97 - 2.19). Based on ERG patterns and clinical examination, a clinical diagnosis of RP (n = 19; 86%), cone-rod dystrophy (CRD; n = 2; 9%), or macular dystrophy (n = 1; 5%) was made. The median self-reported age at onset was 3.0 years (IQR 7.8; range 0.8 - 49.0) and the median disease duration (age at onset subtracted from current age) was 18.7 years (IQR 16.7; range 4.7 - 39.3). An adult onset of symptoms was reported by 2 patients.

Table 1. Summary of the clinical characteristics of patients with *CRB1*-associated retinal dystrophies at last examination.

2.4

Table 1. Summary of the clinical characteristics of patients with *CRB1*-associated retinal dystrophies at last examination. (continued)

Characteristic	Total (n = 22)
Macular dystrophy	1 (5%)
Age at onset in years	
Mean ± SD	8.2 ± 11.9
Median (IQR)	3.0 (7.8)
Range	0.8 to 49.0
Initial symptoms, n (%)	
Nyctalopia	5 (23%)
Visual field loss	8 (36%)
Visual acuity loss	7 (32%)
Nystagmus	2 (9%)
Disease duration in years	
Mean ± SD	19.0 ± 10.7
Median (IQR)	18.7 (16.7)
Range	4.7 to 39.3
Best-corrected visual acuity in ETDRS	
Mean ± SD	38.6 ± 19.7
Median (IQR)	35.8 (27.1)
Range	8.5 to 76.5
SER in diopters	
Mean ± SD	2.2 ± 2.9
Median (IQR)	2.4 (3.9)
Range	-5.9 to 6.7
Axial length in mm ²	
Mean ± SD	21.1 ± 1.7
Median (IQR)	20.8 (1.7)
Range	19.0 to 26.3
V4e isopter seeing retinal areas in mm²	
Mean ± SD	258.6 ± 230.9
Median (IQR)	189.4 (261.7)
Range	14.5 to 744.4
Electroretinography patterns, n (%)	
Normal responses	1 (5%)
Cone-rod pattern	2 (9%)
Minimal responses	1 (5%)
Non-detectable	18 (81%)

Findings were averaged between eyes. ETDRS = Early Treatment Diabetic Retinopathy Study; IQR = Interquartile range; ER = Interquartile

Fifteen different *CRB1* variants were present in this cohort, of which 12 were missense variants, 1 splice-site variant, 1 in-frame deletion, and 1 nonsense variant (Figure 1 and Supplemental Table S1). The most common variant found in this cohort was the founder variant c.3122T>C (p.Met1041Thr), which was present in a homozygous manner

in all 10 patients from the genetic isolate, and in a compound heterozygous manner in 1 patient from outside the isolate. In 10 out 11 patients (91%), including the patient from outside the isolate, this variant caused an early-onset RP phenotype. Patient P10 exhibited a late-onset CRD phenotype, despite originating from the genetic isolate. No other variants were found in patient P10 using targeted next generation sequencing. Additionally, 2 patients with the variant p.(Thr631Cys) in a compound heterozygous manner, showed relative preservation of visual function and retinal structure at later ages compared to other RP patients in this cohort, which was suggestive for a milder form of RP.

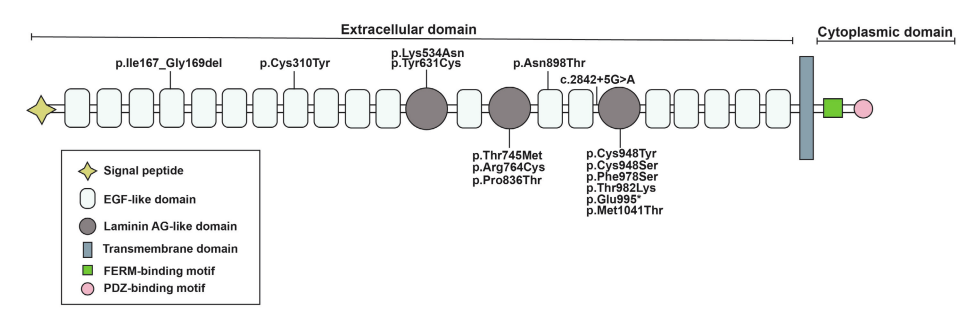


Figure 1. A schematic drawing of the CRB1 protein structure and the variants found in our cohort. The canonical protein CRB1 isoform (NM_201253.2) is comprised of EGF-like domains, laminin AG-like domains, and a short cytoplasmic tail containing FERM and PDF-binding domains. In total, fifteen different variants were found in this cohort, which have all been described previously. The variant p.(Met1041Thr) was the most common variant found in this cohort, which was found in all 10 patients that originated from a Dutch genetic isolate, and in 1 patient from outside the genetic isolate.

Visual acuity and refraction

The mean BCVA of the study eyes was 41.1 ETDRS letters (SD \pm 18.3; range 18.0 to 78.0; equivalent to 0.88 logMAR or 20/150 Snellen) at baseline and 38.6 ETDRS letters (SD \pm 19.7; range 8.5 – 76.5; equivalent to 0.93 logMAR or 20/170 Snellen) at 2-year follow-up. While a trend for a lower ETDRS score at follow-up was observed, this finding was not statistically significant (-2.5 ETDRS letters, 95% CI: -5.2 to 0.2; p = 0.069). A loss of \geq 15 ETDRS letters (i.e. a loss of 3 ETDRS lines) was measured in 5 eyes of 5 patients (11%) at the 2-year follow-up, whose initial ages ranged from 22 to 31 years (Figure 2A). In 2 out of 5 eyes (40%) with a BCVA loss of \geq 15 ETDRS letters, clinical examination showed significant posterior subcapsular cataract at both visits. Patient P1 underwent cataract surgery in both eyes between visits, with no improvement in BCVA. No new cases of cataract were seen at follow-up. Spherical equivalent of the refractive error, excluding pseudophakic patients, did not significantly change between visits (-0.09 D, 95% CI: -0.34 to 0.15; p = 0.455).

Kinetic perimetry and microperimetry

The median size of V4e isopter seeing retinal areas, averaged between both eyes of each individual patient, was 176.0 mm² (IQR 241.9; range 17.7 – 739.2) at baseline. Overall, there was no significant change in V4e seeing retinal areas at the 2-year follow-up visit (-3.5 mm², 95% CI: -17.4 to +10.3; p = 0.616). A loss of \geq 20% in V4e seeing retinal areas was seen in 7 eyes of 6 patients (16%), of whom 2 patients had BCVA-based severe visual impairment (BCVA \leq 35 ETDRS letters). Moreover, 7 eyes of 4 patients showed an increase of \geq 20% in V4e retinal seeing areas from baseline (Figure 2B). These patients all had severe visual impairment based on visual acuity or visual fields (P20, central visual field \leq 10° from point of fixation).

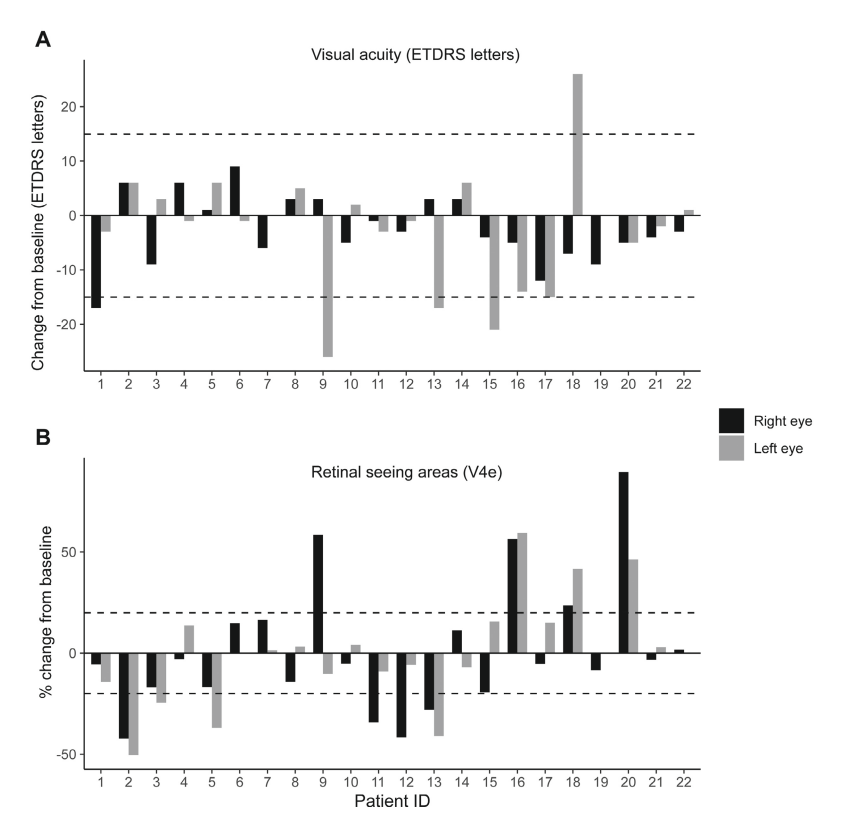


Figure 2. Changes in best-corrected visual acuity (BCVA) using Early Treatment Diabetic Retinopathy Study (ETDRS) letters and visual fields (retinal seeing areas, V4e stimuli) between baseline and 2-year follow-up for each patient. Positive values reflect an improvement from baseline, whereas negative values signify a decrease from baseline. **A**. The absolute change in ETDRS letters was used to illustrate differences from baseline. The threshold for clinical significant BCVA changes was defined as a change of ≥15 ETDRS letters (dashed lines). **B**. For visual fields, the percentage change in retinal seeing areas was used, which was considered clinically significant if it exceeded a 20% change (dashed lines). Patients showing ≥20% improvement in visual field size had severe visual impairment (<35 ETDRS) or severely constricted visual fields (central diameter <20°).

Microperimetry data were available for 36 out of 44 eyes (82%). Microperimetry testing could not be reliably performed in a subset of patients due to age (patients P7, P16) or severe visual impairment (P19, left eye; P20, both eyes). The left eye of patient P2 was also excluded, as this eye was erroneously tested using different threshold settings at follow-up. Figure 3 shows representative microperimetry measurements performed in this cohort. Median BCEA 95% values were 32.9°(SD \pm 49.6; range 1.3 to 187.4) and 44.0° (SD \pm 49.7; range 1.0 to 178.2) for the right and left eyes, respectively. Higher BCEA values, indicating a more unstable fixation, were seen in patients with worse logMAR BCVA (Spearman's $\rho=0.615$; p=0.004). The mean macular sensitivity was 8.5 dB (SD \pm 7.6; range 0.0 – 24.3) and 7.6 dB (SD \pm 7.5; range 0.0 to 26.3) for right and left eyes, accordingly. Macular sensitivity correlated with logMAR BCVA (Spearman's $\rho=-0.734$; p<0.001). In 9 out of 36 eyes (25%), macular sensitivity was ≤ 1 dB (Figure 3, patient P9). Analysis of the microperimetry testing grid (37 testing loci) showed that patients had a mean of with no measurable sensitivity (+3.5 loci, 95% CI: 0.4 to 6.5; p=0.027) at follow-up.

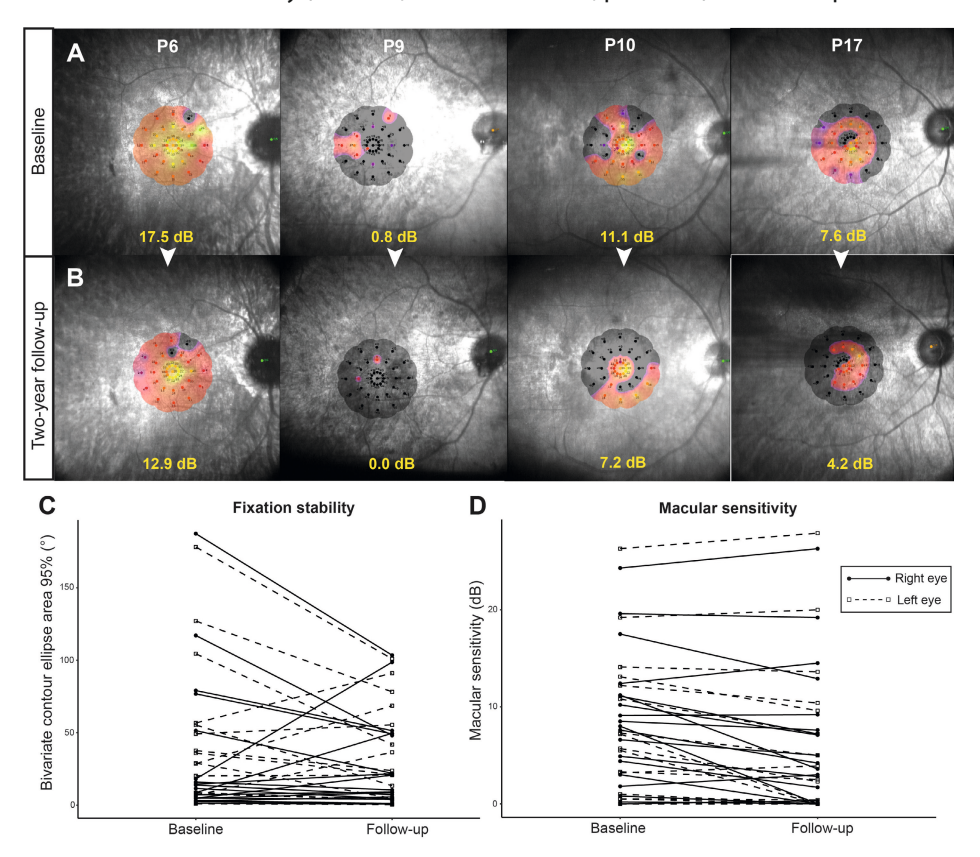


Figure 3. Macular sensitivity (MS) measurements on MAIA microperimetry in patients with *CRB1*-associated retinal dystrophies. Color-coded heat maps are used to demonstrate sensitivity values at each individual loci. Gray regions reflect areas where no sensitivity was measured (absolute scotomas). Mean MS values are

shown in yellow. **A**. MS measurements at baseline in 4 patients with *CRB1*-associated retinal dystrophies. **B**. At 2-year follow-up, MS loss was present in all 4 patients. Note that patient P17 was diagnosed with mild posterior subcapsular cataract, which may contributed to MS loss measured on follow-up. **C**. A spaghetti plot showing longitudinal changes in fixation stability, using bivariate contour ellipse areas (BCEA), in all included study eyes (n = 36). Higher BCEA values signify a more unstable fixation. **D**. A spaghetti plot was also used to illustrate changes in MS for all included study eyes. A significant decline in MS was observed at 2-year follow-up (p < 0.001).

Electroretinography and full-field stimulus testing

Scotopic and photopic responses were minimal or non-recordable at baseline in all patients with RP (Table 1), ERGs in P10 and P21 followed a cone-rod dystrophy pattern, whereas P22 (the patient with a macular dystrophy phenotype) demonstrated full-field scotopic and photopic responses within normal limits. Patients with residual responses showed no significant changes in ERG patterns over follow-up. FST measurements were available for 14 patients (64%) at baseline and available for 20 patients (91%) at follow-up, as FST was not available at the start of this study. Two patients (P2 and P16) were not able to reliably perform FST, most likely due to young age. Therefore, to provide a more accurate and complete overview of FST measurements in this cohort. FST responses from the final visit were used for analysis. The mean thresholds for the white, blue and red stimuli at last visit were -38.6 dB (SD \pm 12.5; range -57.0 to -11.9), -42.7 dB (SD \pm 13.2; range -61.1 to -13.4) and -26.3 dB (SD \pm 8.9; range -40.0 to -10.4), respectively. Sensitivity thresholds for the white stimuli were best preserved in patients with mild RP and cone(-rod) dystrophies (Figure 4A). Based on the difference in thresholds between blue and red stimuli, FST responses in the 40 included eyes were rod-mediated (n = 15; 38%), mixed rod-cone mediated (n = 23; 57%), or conemediated (n = 2:5%) (Figure 4B). Cone-mediated responses could still be detected in both eyes of patient P4 with early-onset RP who had severe visual impairment and severely restricted visual fields. We were also able to determine FST responses in the left eve of patient P19 (light perception BCVA), who still had mixed FST responses. but was nearing cone-mediated vision. In patients with longitudinal FST data (14/20; 67%), we found no significant changes in white (-1.7 dB; 95% Cl:-3.6 to 0.3; p = 0.098), blue (-0.5 dB, 95% CI: -2.6 to 1.5; p = 0.610) or red (-1.0 dB; 95% CI:-2.3 to 0.3; p = 0.132) FST responses.

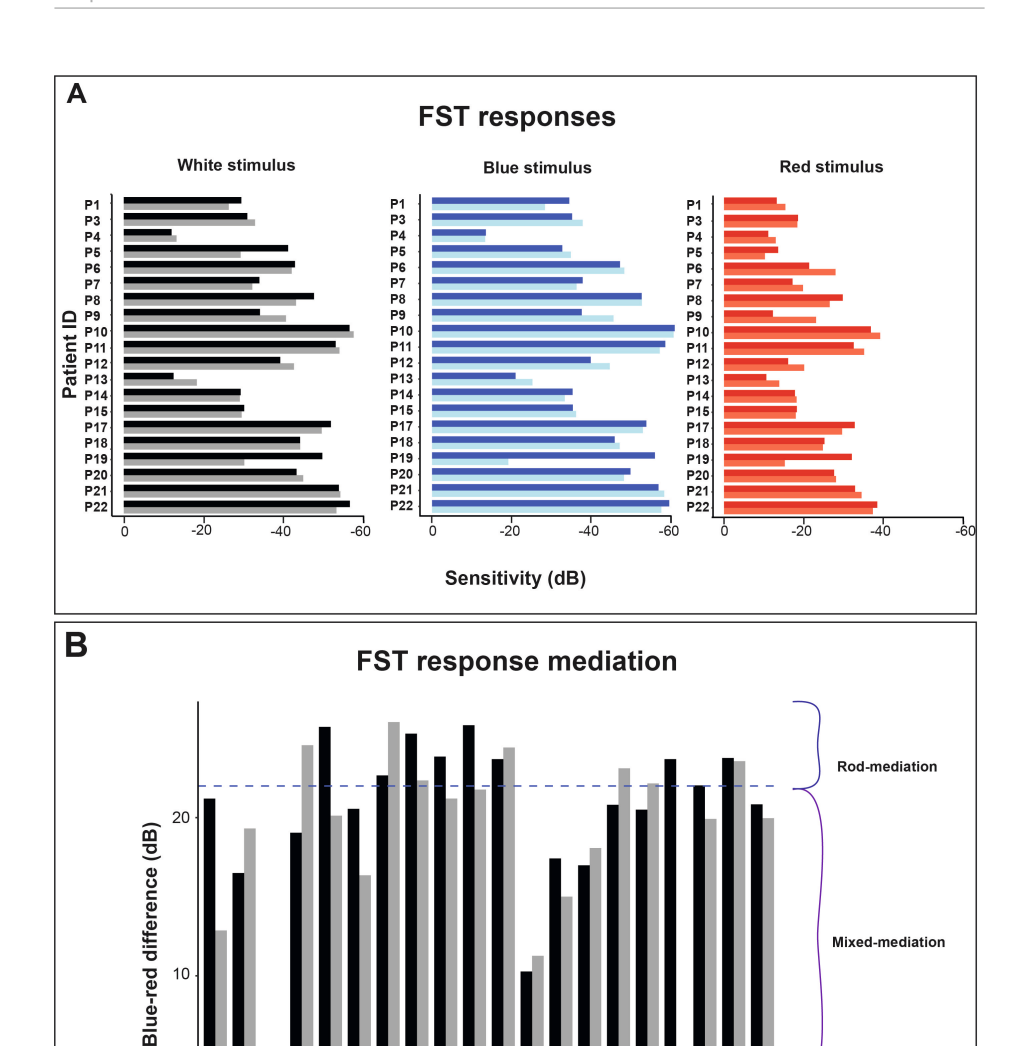


Figure 4. Full-field sensitivity thresholds (FST) responses obtained in 20 patients with *CRB1*-associated retinal dystrophies at 2-year follow-up. Two patients (P2 and P16) were unable to reliably perform FST testing due to young age. **A.** FST responses were obtained using white and chromatic stimuli (blue and red). The grouped bars represent the right eye (darker shaded bars) and left eyes (lighter shaded bars) of a single patient. **B.** Differences between blue and red responses were calculated for each patient. The blue-red difference determined whether FST responses were rod-mediated (difference of >22 dB), cone-mediated (difference <3 dB), or mixed rod-and-cone-mediated (difference between 3 and 22 dB).

P3 P4 P5 P6 P7 P8 P9 P10 P11 P12 P13 P14 P15 P17 P18 P19 P20 P21 P22

Patient ID

Cone-mediation

Retinal imaging

SD-OCT and FAF data were available in 21 of 22 patients (95%), Retinal imaging could not be performed in patient P16 with early-onset RP due to limited cooperation (aged 6) and nystagmus. A common observation seen on SD-OCT was retinal thickening, which was observed in 20 of 21 patients (95%). Cystoid macular edema and/or cystoid spaces were present in 14 eyes of 8 patients at baseline (38%), which resolved completely in 4 eyes (28%) at follow-up without treatment. The mean central retinal thickness at baseline, after exclusion of patients with cystoid macular edema or cysts. was 133.0 μ m (SD \pm 50.9, range 59.5 to 236.0), which did not significantly change at follow-up (-10.31 um, 95% CI: -34.5 to 13.8; p = 0.371). The structure of the inner retina of patients was categorized into 3 different grades; [1] normal organization without coarse lamination (n = 5:24%): [2] normal organization with coarse lamination (n = 8:38%); and [3] relative disorganization with coarse lamination (n = 8; 38%) (Supplemental Figure 1 and Supplemental Table, S2). The hyperreflective outer retinal bands, ELM and EZ, were discontinuous or absent at the (para) fovea and perifovea in 18 of 21 patients (86%, Supplemental Table S2). A degree of preservation of the ELM and EZ integrity was observed in patients with mild RP (P11 and P20), and in the patient with a macular dystrophy phenotype (P22). These 3 patients had better baseline logMAR BCVA (-0.6 logMAR, 95% CI: -1.1 to -0.1; p = 0.015) and macular sensitivity (+13.7 dB, 95% CI: 7.6 to 20.2; p < 0.001) values compared to the other patients in this cohort. Qualitatively, there were no clear changes in ELM and EZ band integrity on SD-OCT imaging at 2-year follow-up examinations, despite a decline in visual acuity in several patients (Figure 5). As the integrity of ELM and EZ layers were severely affected in the majority of patients (e.g. Figure 5A and 5B), quantitative analysis of the retinal bands could not be reliable performed. On FAF imaging, the predominant pattern observed was generalized hypo-autofluorescence in the (mid)peripheral retina, with residual autofluorescence at the central macula, albeit to varying degrees (Figure 5A). FAF imaging was also able to confirm our fundoscopic findings of preserved RPE regions adjacent to retinal arterioles (Figure 5B), Consistent with SD-OCT findings, autofluorescence signals were best preserved in patients with mild RP and macular dystrophy (Figure 5C). The FAF patterns of each patient are described in Supplemental Table S2, which remained unchanged at follow-up.

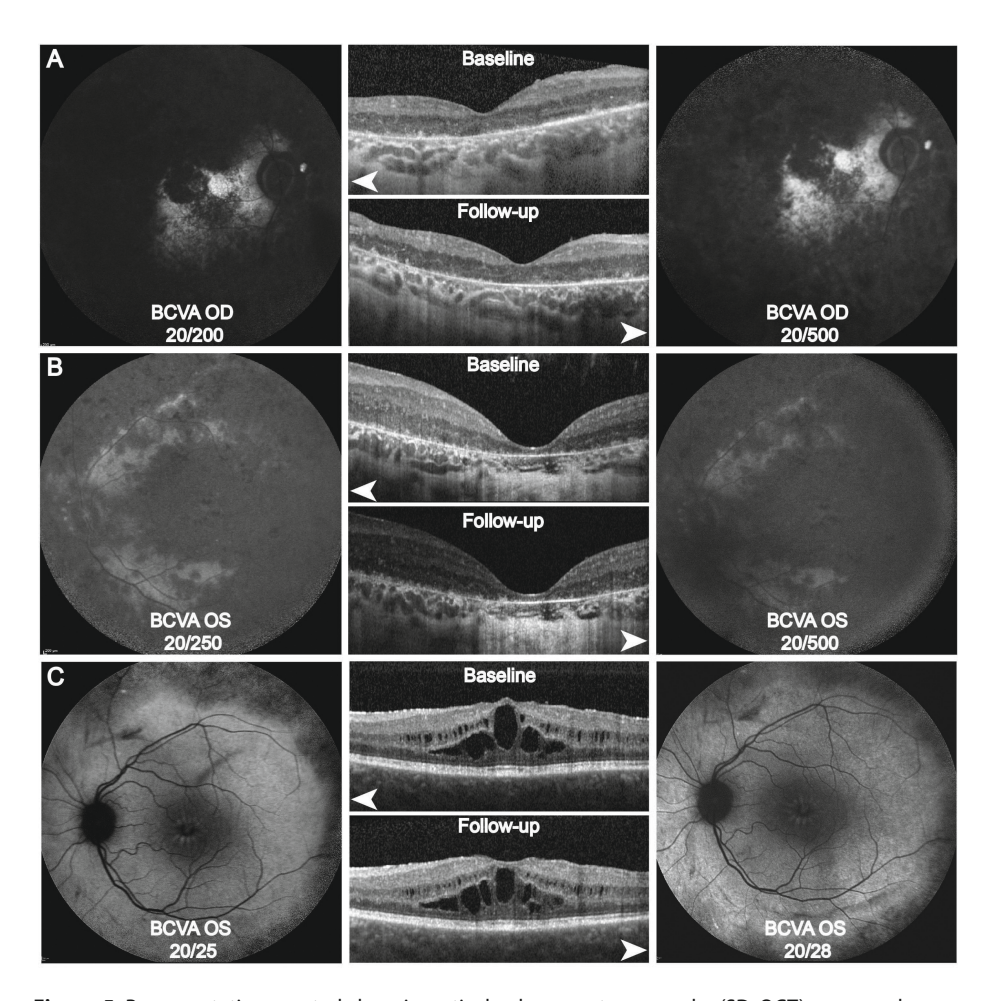


Figure 5. Representative spectral-domain optical coherence tomography (SD-OCT) scans and corresponding fundus autofluorescence (FAF, white arrowheads) images at baseline and at 2-year follow-up in 3 patients with *CRB1*-associated retinitis pigmentosa. Best-corrected visual acuity (BCVA) is shown for each eye in Snellen notation. **A**. Patient P1, aged 30, showed characteristic features of a *CRB1* retina, including inner retinal thickening and coarse lamination of individual retinal layers. Outer retinal bands were nearly absent. FAF imaging in this patient showed overall absence of autofluorescence (AF) in the posterior pole, with some residual AF between the central macula and optic disc. **B**. Patient P13, aged 21, also showed retinal thickening and coarse lamination, in addition to severe foveal atrophy. AF signals were nearly absent, with some preservation of RPE alongside the vascular arterioles. **C**. Patient P11, aged 31, exhibited a mild form of RP. Unlike other RP patients in this cohort, the retinal structure of the inner and outer retina was retained, aside from the presence of cystoid macular edema. Consistent with SD-OCT findings, FAF imaging showed relative preservation of AF in the posterior pole, with signs of degeneration in the (mid)periphery.

DISCUSSION

In this prospective natural history study, we evaluated the functional and structural changes in patients with biallelic CRB1 variants causing a spectrum of retinal dystrophies, as we anticipate the start of gene therapeutic trials for CRB1-associated RDs in the near future. Our two-year analysis of the cohort showed that visual acuity and visual fields did not significantly change during follow-up. BCVA and visual fields are parameters with relatively low sensitivity for early disease changes, and may not be suitable as primary outcome measures in clinical trials on diseases that have relatively slow progression rates, such as RP.33 Still, in 5 eyes of 5 different patients, aged between 22 and 31 years, we found a BCVA loss of more than 15 ETDRS letters (equivalent to +0.3 logMAR), which is considered a clinically significant change in clinical trials and by regulatory agencies. 34,35 This finding suggests a faster decline around the 3rd decade of life, although the contribution of significant cataract, which was the case for 2 out of 5 eyes, should not be disregarded. This is in line with our retrospective natural history study, which reported median ages of 18, 32, and 44 years to reach moderate visual impairment, severe visual impairment, and blindness, respectively.¹⁸ Based on BCVA data, we suggest that the optimal window for treatment is before the 3rd decade of life. Ideally, patients should be treated at the earliest and safest opportunity to gain the most benefit from gene therapy.

Regarding visual fields, we found that 7 eyes of 6 patients showed progression within the 2-year follow-up period, defined as a loss of ≥20% of the seeing retinal area, which is the test-retest limit in RP patients as found by Bittner and collagues.²⁶ However, these changes should be interpreted with caution, as greater variability in visual field measurements is predicted in patients with more advanced stages of BCVA- or visual field-based impairment.³⁶⁻³⁸ This is evidently demonstrated in our cohort as 4 severe visually impaired patients showed improvements up to 90% in visual fields areas at follow-up, in absence of intervention. Goldmann kinetic perimetry assumes stable and foveal fixation, which is not always the case in patients with severe RP such as in the current study.²⁶ Instead, other perimetry modalities, such as semi-automated kinetic perimetry or wide-field static perimetry, could be used in future studies for peripheral visual field assessment, as they take fixation stability into consideration and limit operator-dependent variability.³⁹

Fundus-tracking perimetry, also known as microperimetry, is a commonly used tool for monitoring disease progression and for assessing treatment efficacy in trials involving other RDs, such as Stargardt disease, choroideremia and X-linked RP.^{32, 40, 41, 42} In these RDs, subtle changes in the retina over short periods of time were detectable on microperimetry, preceding detection on conventional parameters.^{27, 43} Similar results were found in our cohort, in which we detected a significant decline in macular sensitivity between visits, while no significant decline in BCVA was detected

in the 2-year period. Thus, microperimetry is a sensitive progression marker, and has the potential to serve as a clinical endpoint in treatment trials for CRB1-associated RD. However, due to the subjective nature of psychophysical metrics, measurements on microperimetry are inherently susceptible to variability, which is affected by factors including age, the type of retinal disease, disease severity, learning effects, and natural variance. 27,44 While our study accounted for potential learning effects. formal intrasession and intersession reliability testing was not performed. As the main goal of phase III gene therapy trials is treatment efficacy, a patient's ability to reliably perform microperimetry testing could potentially be an inclusion criterion. Analysis of microperimetry was also impeded by the increasing amount of absolute scotoma points, which resulted in nearly undetectable sensitivity thresholds (macular sensitivity ≤1 dB) in 25% of the study eyes. Reporting the macular sensitivity, which is calculated using the average sensitivity of all testing loci, may not be an ideal approach, as this underestimates the change occurring in individual loci with detectable sensitivity. 27, 40, ⁴⁵ Other methods that investigate regional sensitivity changes, along with test-retest reliability testing, should be explored in future studies.44

On electrophysiological testing, ERG responses were non-recordable in the majority of RP patients, implying that ffERG has no value in monitoring disease progression in patients with CRB1-associated RP. An alternative approach to assess residual photoreceptor function is the measurement of sensitivity thresholds using FST, which can be performed regardless of fixation capabilities or ERG function.⁴⁶ FST testing showed rod or mixed responses in this cohort, which shows that functional photoreceptors are still present despite this severe early-onset disease. Cone-mediated responses were found in patient P4, which is suggestive for end-stage disease as these responses are typically found in patients with a LCA phenotype. 13,47 As such, FST can provide valuable knowledge on remaining photoreceptor function, and in turn, disease severity, which can guide the selection of eligible candidates for therapeutic intervention.³² However, FST responses do not appear to be sensitive markers for disease progression over a relatively short period, as we found no significant changes in FST responses over the course of 2 years. Small, localized changes occurring over several years possibly go unnoticed, as FST measures the sensitivity of the entire retina, without revealing spatial information.³⁰ Nevertheless, FST is potentially capable of measuring a treatment effect, as shown in previous gene therapy trials, and should be considered as a clinical endpoint.⁴⁸⁻⁵⁰

In keeping with previous studies, SD-OCT imaging in patients with *CRB1*-associated RP revealed an abnormally thickened inner retina (95%), which could be accompanied by coarse lamination of inner retinal layers and/or cystoid macular edema.^{11, 17, 18} It has been postulated that the loss of CRB1 function stimulates proliferation of retinal progenitor cells, and also disrupts naturally occurring apoptosis during retinal development.^{9,} This phenomenon is in direct contrast with other molecular forms of RP/LCA,

where progressive thinning of the inner retinal layers typically occurs. 51 Regardless of inner retinal thickening, most patients (62%) showed a relatively preserved laminar organization, which may be amenable for gene therapy treatment. The hyperreflective retinal bands, ELM and EZ, were typically discontinuous or indiscernible, consistent with FAF findings, owing to the rapid disease progression at an early age in CRB1associated RP, which impeded quantitative analysis.51 Despite the state of the inner and outer retina, retinal sensitivity could still be measured using psychophysical metrics, indicating that SD-OCT findings do not necessarily reflect remaining photoreceptor function in patients with CRB1-associated RDs. There is an urgent need for reliable methods for accurate quantification and localization of remaining photoreceptors, as viable photoreceptors are a prerequisite for effective treatment with gene therapy. 53, 54,55 A potential method is the use of adaptive optics, as it allows for the assessment of photoreceptor viability on a cellular level, which, in turn, can shed light on their amenability for gene therapy treatment. 55,56,57 It would be of great interest to assess in future studies whether photoreceptors can be adequately identified using adaptive optics considering the severe, early-onset degeneration and the characteristic retinal phenotype seen in CRB1 patients.

Our study has several limitations. We included a relatively small cohort of 22 patients with *CRB1*-associated retinal dystrophies, which limited the possibility of a more indepth (subgroup) analysis. Furthermore, as patients were observed over a period of 2 years, it is possible that parameters with low sensitivity for disease progression in our current study, such as visual acuity and FST, will be able to demonstrate progression over a longer observation period. Novel outcome measurements used in the assessment of gene therapy, such as multi-luminance mobility tests, dark-adapted chromatic perimetry and pupil campimetry, were also not assessed in this study.^{58,59} Future studies that follow a large group of patients with *CRB1* variants over a longer period of time, while also assessing the feasibility of more recent outcome measures, would be invaluable to extend our current findings.

In conclusion, this is the first prospective natural history study performed in patients with RDs associated with biallelic *CRB1* variants. Our study discusses the feasibility of commonly used outcome measures as clinical endpoints in clinical trials, and their potential caveats. BCVA and visual fields measures show stability over 2 years and need to be complemented with more sensitive progression markers. Microperimetry and FST show most potential as clinical endpoints, but further investigation into their reliability, validity and feasibility is required. The findings in this study can be used to aid the design of interventional studies, paving the way for *CRB1* gene therapy trials in the near future

ACKNOWLEDGEMENTS

LIVdB, CBH and CJFB are members of the European Reference Network for Rare Eye diseases (ERN-EYE).

Funding/Support

This research was supported by the following organizations: Algemene Nederlandse Vereniging ter Voorkoming van Blindheid (ANVVB), Landelijke Stichting voor Blinden en Slechtzienden (LSBS), and the Oogfonds, which contributed through UitZicht (Delft, the Netherlands); as well as the Curing Retinal Blindness Foundation, Stichting Blindenhulp, Bontius Stichting, and Retina Fonds. These funding organizations had no role in the design or conduct of this research.

Financial disclosure

The Leiden University Medical Center (LUMC) is the holder of patent application PCT/ NL2014/050549, which describes the potential clinical use of CRB2; JW is listed as inventor on this patent, and JW is an employee of the LUMC.

RFFFRFNCFS

- 1. Khan KN, Robson A, Mahroo OAR, et al. A clinical and molecular characterisation of CRB1-associated maculopathy. *Eur J Hum Genet*. 2018;26(5):687-694.
- 2. Vincent A, Ng J, Gerth-Kahlert C, et al. Biallelic Mutations in CRB1 Underlie Autosomal Recessive Familial Foveal Retinoschisis. *Investigative Ophthalmology & Visual Science*. 2016;57(6):2637-2646.
- 3. Lotery AJ, Jacobson SG, Fishman GA, et al. Mutations in the CRB1 Gene Cause Leber Congenital Amaurosis. *Archives of Ophthalmology*. 2001;119(3):415-420.
- 4. den Hollander AI, Heckenlively JR, van den Born LI, et al. Leber congenital amaurosis and retinitis pigmentosa with Coats-like exudative vasculopathy are associated with mutations in the crumbs homologue 1 (CRB1) gene. *American journal of human genetics*. 2001;69(1):198-203.
- 5. Verbakel SK, van Huet RAC, Boon CJF, et al. Non-syndromic retinitis pigmentosa. *Progress in Retinal and Eye Research*. 2018;66:157-186.
- 6. Hartong DT, Berson EL, Dryja TP. Retinitis pigmentosa. The Lancet. 2006;368(9549):1795-1809.
- Quinn PM, Buck TM, Mulder AA, et al. Human iPSC-Derived Retinas Recapitulate the Fetal CRB1 CRB2 Complex Formation and Demonstrate that Photoreceptors and Müller Glia Are Targets of AAV5. Stem Cell Reports. 2019;12(5):906-919.
- 8. Quinn PM, Pellissier LP, Wijnholds J. The CRB1 Complex: Following the Trail of Crumbs to a Feasible Gene Therapy Strategy. *Front Neurosci.* 2017:11:175.
- 9. Alves CH, Pellissier LP, Wijnholds J. The CRB1 and adherens junction complex proteins in retinal development and maintenance. *Progress in Retinal and Eve Research*. 2014:40:35-52.
- 10. Boon N, Wijnholds J, Pellissier LP. Research Models and Gene Augmentation Therapy for CRB1 Retinal Dystrophies. *Front Neurosci.* 2020;14:860.
- 11. Bujakowska K, Audo I, Mohand-Saïd S, et al. CRB1 mutations in inherited retinal dystrophies. *Hum Mutat*. 2012;33(2):306-315.
- 12. Ray TA, Cochran K, Kozlowski C, et al. Comprehensive identification of mRNA isoforms reveals the diversity of neural cell-surface molecules with roles in retinal development and disease. *Nat Commun.* 2020;11(1):3328-3328.
- 13. Stingl KT, Kuehlewein L, Weisschuh N, et al. Chromatic Full-Field Stimulus Threshold and Pupillography as Functional Markers for Late-Stage, Early-Onset Retinitis Pigmentosa Caused by CRB1 Mutations. *Transl Vis Sci Technol.* 2019:8(6):45-45.
- 14. Alves CH, Boon N, Mulder AA, Koster AJ, Jost CR, Wijnholds J. CRB2 Loss in Rod Photoreceptors Is Associated with Progressive Loss of Retinal Contrast Sensitivity. *Int J Mol Sci.* 2019;20(17).
- 15. Pellissier LP, Quinn PM, Alves CH, et al. Gene therapy into photoreceptors and Müller glial cells restores retinal structure and function in CRB1 retinitis pigmentosa mouse models. *Human Molecular Genetics*. 2015;24(11):3104-3118.
- Mehalow AK, Kameya S, Smith RS, et al. CRB1 is essential for external limiting membrane integrity and photoreceptor morphogenesis in the mammalian retina. *Human Molecular Genetics*. 2003;12(17):2179-2189.
- 17. Jacobson SG, Cideciyan AV, Aleman TS, et al. Crumbs homolog 1 (CRB1) mutations result in a thick human retina with abnormal lamination. *Human Molecular Genetics*. 2003;12(9):1073-1078.
- 18. Talib M, van Schooneveld MJ, van Genderen MM, et al. Genotypic and phenotypic characteristics of *CRB1*-associated retinal dystrophies. *Ophthalmology*. 2017;124(6):884-895.

- 19. Buck TM, Vos RM, Alves CH, Wijnholds J. AAV-CRB2 protects against vision loss in an inducible CRB1 retinitis pigmentosa mouse model. *Molecular Therapy Methods & Clinical Development*. 2021;20:423-441
- 20. Talib M, Boon CJF. Retinal Dystrophies and the Road to Treatment: Clinical Requirements and Considerations. *The Asia-Pacific Journal of Ophthalmology*, 2020;9(3).
- Mathijssen IB, Florijn RJ, van den Born LI, et al. LONG-TERM FOLLOW-UP OF PATIENTS WITH RETINITIS
 PIGMENTOSA TYPE 12 CAUSED BY CRB1 MUTATIONS: A Severe Phenotype With Considerable
 Interindividual Variability. *Reting*, 2017;37(1):161-172.
- 22. van Huet RAC, Oomen CJ, Plomp AS, et al. The RD5000 Database: facilitating clinical, genetic, and therapeutic studies on inherited retinal diseases. *Investigative Ophthalmology & Visual Science*. 2014:55(11):7355-7360.
- 23. van den Born LI, van Soest S, van Schooneveld MJ, Riemslag FCC, de Jong PTVM, Bleeker-Wagemakers EM. Autosomal Recessive Retinitis Pigmentosa With Preserved Para-arteriolar Retinal Pigment Epithelium. *American Journal of Ophthalmology*. 1994;118(4):430-439.
- 24. Talib M, van Schooneveld MJ, Wijnholds J, et al. Defining inclusion criteria and endpoints for clinical trials: a prospective cross-sectional study in CRB1-associated retinal dystrophies. *Acta Ophthalmologica*. 2021;*Epub ahead of print*.
- 25. Dagnelie G. Technical note. Conversion of planimetric visual field data into solid angles and retinal areas. *Clinical Vision Science*. 1990;5(1):95-100.
- 26. Bittner AK, Iftikhar MH, Dagnelie G. Test-Retest, Within-Visit Variability of Goldmann Visual Fields in Retinitis Pigmentosa. *Investigative Ophthalmology & Visual Science*. 2011;52(11):8042-8046.
- Wu Z, Ayton LN, Guymer RH, Luu CD. Intrasession Test–Retest Variability of Microperimetry in Age-Related Macular Degeneration. *Investigative Ophthalmology & Visual Science*. 2013;54(12):7378-7385.
- 28. Talib M, Jolly JK, Boon CJF. Measuring Central Retinal Sensitivity Using Microperimetry. In: Boon CJF, Wijnholds J, eds. *Retinal Gene Therapy: Methods and Protocols*. New York, NY: Springer New York; 2018-330-340
- 29. Roman AJ, Cideciyan AV, Aleman TS, Jacobson SG. Full-field stimulus testing (FST) to quantify visual perception in severely blind candidates for treatment trials. *Physiological Measurement*. 2007;28(8):N51-N56.
- 30. Roman AJ, Schwartz SB, Aleman TS, et al. Quantifying rod photoreceptor-mediated vision in retinal degenerations: dark-adapted thresholds as outcome measures. *Experimental Eye Research*. 2005;80(2):259-272.
- 31. Klein M, Birch DG. Psychophysical assessment of low visual function in patients with retinal degenerative diseases (RDDs) with the Diagnosys full-field stimulus threshold (D-FST). *Documenta Ophthalmologica*. 2009;119(3):217.
- 32. Dimopoulos IS, Tseng C, MacDonald IM. Microperimetry as an Outcome Measure in Choroideremia Trials: Reproducibility and Beyond. *Investigative Ophthalmology & Visual Science*. 2016;57(10):4151-4161.
- 33. Fishman GA, Jacobson SG, Alexander KR, et al. Outcome measures and their aplication in clinical trials for retinal degenerative diseases: Outline, Review, and Perspective. *RETINA*. 2005;25(6).
- 34. Lam BL, Feuer WJ, Schiffman JC, et al. Trial end points and natural history in patients with G11778A Leber hereditary optic neuropathy: preparation for gene therapy clinical trial. *JAMA ophthalmology*. 2014;132(4):428-436.
- 35. Kiser AK, Mladenovich D, Eshraghi F, Bourdeau D, Dagnelie G. Reliability and Consistency of Visual Acuity and Contrast Sensitivity Measures in Advanced Eye Disease. *Optometry and Vision Science*. 2005;82(11).

- 36. Barnes CS, Schuchard RA, Birch DG, et al. Reliability of Semiautomated Kinetic Perimetry (SKP) and Goldmann Kinetic Perimetry in Children and Adults With Retinal Dystrophies. *Transl Vis Sci Technol.* 2019;8(3):36-36.
- 37. Barry MP, Bittner AK, Yang L, Marcus R, Iftikhar MH, Dagnelie G. Variability and Errors of Manually Digitized Goldmann Visual Fields. *Optometry and vision science : official publication of the American Academy of Optometry*. 2016;93(7):720-730.
- Roman AJ, Cideciyan AV, Schwartz SB, Olivares MB, Heon E, Jacobson SG. Intervisit Variability of Visual Parameters in Leber Congenital Amaurosis Caused by RPE65 Mutations. *Investigative Ophthalmology* & Visual Science. 2013:54(2):1378-1383.
- 39. Kumaran N, Rubin GS, Kalitzeos A, et al. A Cross-Sectional and Longitudinal Study of Retinal Sensitivity in RPE65-Associated Leber Congenital Amaurosis. *Investigative ophthalmology & visual science*. 2018;59(8):3330-3339.
- Schönbach EM, Strauss RW, Muñoz B, et al. Longitudinal Microperimetric Changes of Macular Sensitivity in Stargardt Disease After 12 Months: ProgStar Report No. 13. JAMA Ophthalmology. 2020;138(7):772-779.
- 41. Georgiou M, Singh N, Kane T, et al. Long-Term Investigation of Retinal Function in Patients with Achromatopsia. *Investigative ophthalmology & visual science*. 2020;61(11):38-38.
- 42. Buckley TMW, Jolly JK, Menghini M, Wood LJ, Nanda A, MacLaren RE. Test-retest repeatability of microperimetry in patients with retinitis pigmentosa caused by mutations in RPGR. *Clinical & Experimental Ophthalmology*. 2020;48(5):714-715.
- 43. Jolly JK, Xue K, Edwards TL, Groppe M, MacLaren RE. Characterizing the Natural History of Visual Function in Choroideremia Using Microperimetry and Multimodal Retinal Imaging. *Investigative Ophthalmology & Visual Science*. 2017;58(12):5575-5583.
- 44. Pfau M, Jolly JK, Wu Z, et al. Fundus-controlled perimetry (microperimetry): Application as outcome measure in clinical trials. *Progress in Retinal and Eye Research*. 2020:100907.
- 45. Iftikhar M, Kherani S, Kaur R, et al. Progression of Retinitis Pigmentosa as Measured on Microperimetry: The PREP-1 Study. *Ophthalmology Retina*. 2018;2(5):502-507.
- 46. Maguire AM, High KA, Auricchio A, et al. Age-dependent effects of RPE65 gene therapy for Leber's congenital amaurosis: a phase 1 dose-escalation trial. *Lancet*. 2009;374(9701):1597-1605.
- 47. Collison FT, Park JC, Fishman GA, McAnany JJ, Stone EM. Full-Field Pupillary Light Responses, Luminance Thresholds, and Light Discomfort Thresholds in CEP290 Leber Congenital Amaurosis Patients. *Investigative Ophthalmology & Visual Science*. 2015;56(12):7130-7136.
- 48. Russell S, Bennett J, Maguire AM, High KA. Voretigene neparvovec-rzyl for the treatment of biallelic RPE65 mutation—associated retinal dystrophy. *Expert Opinion on Orphan Drugs*. 2018;6(8):457-464.
- 49. Russell S, Bennett J, Wellman JA, et al. Efficacy and safety of voretigene neparvovec (AAV2-hRPE65v2) in patients with RPE65-mediated inherited retinal dystrophy: a randomised, controlled, open-label, phase 3 trial. *Lancet*. 2017;390(10097):849-860.
- 50. Klein M, Mejia P, Galles D, Birch DG. Full-Field Stimulus Thresholds (FSTs) in Subjects with Inherited Retinal Degenerations (IRDs) a 10 Years Review. *Investigative Ophthalmology & Visual Science*. 2018;59(9):54-54.
- 51. Tee JJL, Yang Y, Kalitzeos A, Webster A, Bainbridge J, Michaelides M. Natural History Study of Retinal Structure, Progression, and Symmetry Using Ellipzoid Zone Metrics in RPGR-Associated Retinopathy. American Journal of Ophthalmology. 2019;198:111-123.
- 52. Bouzia Z, Georgiou M, Hull S, et al. GUCY2D-Associated Leber Congenital Amaurosis: A Retrospective Natural History Study in Preparation for Trials of Novel Therapies. *American journal of ophthalmology*. 2020;210:59-70.

- 53. Gardiner KL, Cideciyan AV, Swider M, et al. Long-Term Structural Outcomes of Late-Stage RPE65 Gene Therapy. *Molecular Therapy*. 2020;28(1):266-278.
- 54. Aguirre GD. Concepts and Strategies in Retinal Gene Therapy. *Investigative ophthalmology & visual science*, 2017;58(12):5399-5411.
- 55. Georgiou M, Kalitzeos A, Patterson EJ, Dubra A, Carroll J, Michaelides M. Adaptive optics imaging of inherited retinal diseases. *The British journal of ophthalmology*. 2018:102(8):1028-1035.
- 56. Genead MA, Fishman GA, Rha J, et al. Photoreceptor structure and function in patients with congenital achromatopsia. *Investigative ophthalmology & visual science*. 2011;52(10):7298-7308.
- 57. Georgiou M, Fujinami K, Michaelides M. Inherited retinal diseases: Therapeutics, clinical trials and end points—A review. *Clinical & Experimental Ophthalmology*. 2021;49(3):270-288.
- 58. Stingl K, Kempf M, Bartz-Schmidt KU, et al. Spatial and temporal resolution of the photoreceptors rescue dynamics after treatment with voretigene neparvovec. *British Journal of Ophthalmology*. 2021:bjophthalmol-2020-318286.
- 59. Maguire AM, Russell S, Wellman JA, et al. Efficacy, Safety, and Durability of Voretigene Neparvovecrzyl in RPE65 Mutation–Associated Inherited Retinal Dystrophy: Results of Phase 1 and 3 Trials. *Ophthalmology*. 2019;126(9):1273-1285.

SUPPLEMENTAL CONTENT

 Table S1. Patient's clinical and genetic characteristics at baseline in the CRB1 cohort

Allele 1; Allele 2 Dx Age at First ETDRS onset symptom BCVA	Dx Age at First onset symptom	Dx Age at First onset symptom	First symptom	First symptom	ETDRS BCVA	i	SER ©	Axial length	Lens status	ERG pattern	V4e (mm²)		Fundus features	atures	
(6)	(À	3	(×)					Œ E	(SO/QO)			Vitreous	ONH	Bone- spicules	PPRPE
p.(Met1041Thr); RP 6 VF loss p.(Met1041Thr)	RP 6	9		VFloss		47.5	+0.6	21.4	PSC	QN O	156.3	Vitreous	>	>	×
p.(Met1041Thr); RP 1-2 Nyctalopia p.(Met1041Thr)	RP 1-2	1-2		Nyctalopi	в	39.5	+3.1	19.8	Clear	Q.	35.4	Vitreous cells	>	>	>
p.(Met1041Thr); RP 1 VFloss p.(Met1041Thr)	, RP 1	-	1 VFloss	VF loss		54.0	+0.6	20.8	Clear	Q.	140.2	Vitreous cells	×	>	>
p.(Met1041Thr); RP <1 Nyctalopia p.(Met1041Thr)	. RP <1	▽		Nyctalopi	æ	31.5	+1.0	20.7	PSC	QN	36.4	Clear	×	>	>
p.(Met1041Thr); RP 2 VF loss p.(Met1041Thr)	, RP 2	2		VFloss		26.5	+3.9	21.3	PSC	QN	82.7	Vitreous cells	>	>	×
p.(Met1041Thr); RP 3 VF loss p.(Met1041Thr)	RP 3	æ		VFloss		0.09	+3.2	19.5	Clear	QN	278.5	Vitreous cells	>	>	>
p.(Met1041Thr); RP 2 Nystagmus p.(Met1041Thr)	RP 2	2		Nystagmu	2	19.0	+6.7	19.1	Clear	QN	275.7	Clear	×	>	×
p.(Met1041Thr); RP 3 VF loss p.(Met1041Thr)	; RP 3	m		VFloss		26.5	+7.1	19.5	Clear	MR	537.4	PRH	×	>	>
p.(Met1041Thr); RP 8 VF loss p.(Met1041Thr)	RP 8	80		VF loss		20.0	+5.8	20.6	Clear	ND	174.5	Asteroid hyalosis	>	>	>
p.(Met1041Thr); CRD 34-35 VA loss p.(Met1041Thr)	CRD 34-35	34-35		VA loss		78.0	+2.5	21.4	Clear	CRD	729.4	Vitreous veils	>	>	×
p.(Tyr631Cys); MildRP 7-8 VA loss p.(Glu995*)	MildRP 7-8	7-8		VA loss		75.5	+1.0	21.7	Clear	ND	324.6	Vitreous cells	×	>	×
p.(Asn898Thr); RP 9 VA loss p.(Asn898Thr)	RP 9	6		VA loss	1	57.0	4.1+	20.9	Clear	ON I	312.5	Vitreous cells	> !	> !	> !

Table S1. Patient's clinical and genetic characteristics at baseline in the CRB1 cohort (continued)

₽	Age, Sex	Allele 1; Allele 2	ă	Age at onset (y)	First symptom	ETDRS BCVA	SER (D)	Axial length (mm)	Lens status (OD/OS)	ERG pattern	V4e (mm²)		Fundus features	eatures	
												Vitreous	ONH	Bone-	PPRPE
													drusen	spicules	
P13	P13 M, 21	p.(Cys948Tyr); p.(Met1041Thr)	RP	2	Nyctalopia	21.0	+2.6	19.9	PSC	QN	202.5	Vitreous	×	>	>
P14	F, 24	p.(Arg764Cys); p.(Glu995*)	RP PP	7	Nyctalopia	36.0	+5.3	19.4	PSC	ND	82.3	Clear	×	>	×
P15	F, 31	p.(Arg764Cys); p.(Glu995*)	RP.	-	Nyctalopia	41.5	+4.8	19.2	Clear	QN	160.7	Vitreous	×	>	>
P16	M, 6	p.(Cys310Tyr); p.(Phe978Ser)	PP PP	1-2	Nystagmus	18.0	+3.4	20.6	Clear	QN	177.6	Clear	×	>	×
P17	M, 23	p.(Tyr631Cys); p.(Cys948Tyr)	RP	12	VA loss	45.0	-0.6 ^b	22.8	PF/PSC	QN	450.9	No vitreous ^c	×	>	×
P18	F, 12	p.(Thr745Met); c.2842+5G>A	AP.	m	VF loss	29.5	+5.0	20.3	Clear	QN	125.9	Vitreous cells	×	>	>
P19	M, 53	p.(Lys534Asn); p.(Thr745Met)	AP	17	VAloss	27.5	+0.3 ^b	21.5	PF/PF	ND	16.7	No vitreous ^c	×	>	×
P20	M, 74	p.(Tyr631Cys); p.(Thr982Lys)	MildRP	46	VF loss	66.5	-0.8 ^b	24.3	PF/PF	ND	19.1	Vitreous cells	×	>	×
P21	F, 31	p.(Pro836Thr); p.(Cys948Ser)	CRD	4	VA loss	30.5	+0.9	22.2	Clear	CRD	710.1	Clear	×	>	×

The mutation notation is based on the NM_201253.2 nomenclature. Patients P1-P10 originate from the same genetic isolate who were all homozygous carriers of the structure compared to other patients in this cohort. Measurements were averaged between eyes. CRD = cone-rod dystrophy; Dx = diagnosis; MD = macular dystrophy; MR = minimal responses; ND = non-detectable; ONH = optic nerve head; PF = pseudophakic; PPRPE = para-arteriolar preservation of the retinal pigment epithelium; PRH = pre-retinal hemorrhage; PSC = posterior subcapsular cataract; RP = retinitis pigmentosa; RCD = rod-cone dystrophy; SER = spherical refractive error; V4e = V4e retinal seeing areas derived received immediate peripheral laser iridotomy. ^b Patients underwent cataract surgery prior to the baseline visit. Patients underwent pars plana vitrectomy with inner limiting p.(Met1041Th) mutation. Patients P14 and P15 are siblings. Patients P11 and P22 had milder forms of retinitis pigmentosa, as they had better preserved visual acuity and retinal from Goldmann kinetic perimetry; VA = visual acuity; VF = visual field. Patient P15 developed acute-angle closure glaucoma during mydriatic dark-adaption at baseline, and membrane peeling due to cystoid macular edema.

 Table 2.
 Retinal imaging findings in patients with CRB1-associated retinal dystrophies.

□	SD-OCT: retinal architecture	larchitecture	SD	SD-OCT: integrity of outer retinal bands	outer retinal bar	spu	
	Laminar organization Presence of CME	Presence of CME	Paraf	Parafovea	Perifovea	ovea	Fundus autofluorescence
			EZ	ELM	EZ	ELM	
P1	Normal organization	No CME	Discontinuous	Discontinuous	Indiscernible	Discontinuous	Optic nerve drusen, mottled hypo-AF
							fovea and optic disc
P2	Disorganization	CMEODS	Indiscernible	Discontinuous	Indiscernible	Discontinuous	Optic nerve drusen, generalized hypo-
8	Normal organization	Parafoveal cysts	Discontinuous	Discontinuous	Discontinuous	Discontinuous	Ar with residual Ar at the loved Generalized hypo-AF
P4	with coarse lamination Disorganization	No CME	Discontinuous	Discontinuous	Discontinuous	Discontinuous	Generalized hypo-AF
PS	Disorganization	No CME	Discontinuous	Discontinuous	Discontinuous	Discontinuous	Optic nerve drusen, generalized
P6	Disorganization	CME ODS; resolved at	Discontinuous	Discontinuous	Discontinuous	Discontinuous	hypo-AF Optic nerve drusen; hypo-AF with
	1	dn-wollo					residual AF at central macula
Ь7	Disorganization	No CME	Discontinuous	Discontinuous	Discontinuous	Discontinuous	Generalized hypo-AF
P8	Disorganization	CMEODS	Discontinuous	Indiscernible	Discontinuous	Discontinuous	Generalized hypo-AF with hyper-AF
							speckles
Ь6	Normal with coarse	Parafoveal cysts OD;	Indiscernible	Discontinuous	Discontinuous	Discontinuous	Optic drusen, mottled hypo-AF
	lamination	resolved at follow-up					in central macula with relatively
	:		i		i	i	preservation in perimacula
P10	Normal with coarse	Parafoveal cysts OD;	Discontinuous	Discontinuous	Discontinuous	Discontinuous	Perimacular hypo-AF ring with foveal
5	lamination	resolved at follow-up					sparing
_	Notifial Organization	CME OS	Collelladas	Collillidods	Collinations	Collinations	NOTITIAL AF III LITE DOSTETIOI DOTE WILLI
P12	Normal with coarse	CME ODS; CME OS	Discontinuous	Discontinuous	Discontinuous	Discontinuous	Optic nerve drusen, mottled hypo-AF
	lamination	resolved at follow-up					in the periphery and central macula
!			1 1 1 1 1 1 1 1	1 1 1 1 1 1	! ! ! ! !	1 1 1 1 1 1 1 1 1 1 1 1 1 1 1 1 1 1 1 1	with preservation of the perimacula

 Table 2. Retinal imaging findings in patients with CRB7-associated retinal dystrophies. (continued)

۵	SD-OCT: retinal architecture	architecture	-OS	OCT: integrity of	SD-OCT: integrity of outer retinal bands	spu	
	Laminar organization Presence of CME	Presence of CME	Parafovea	ovea	Perifovea	ovea	Fundus autofluorescence
			EZ	ELM	EZ	ELM	
P13	Normal organization	No CME	Discontinuous Discontinuous	Discontinuous	Discontinuous Discontinuous	Discontinuous	Generalized hypo-AF with AF
	and lamination						preservation around the vascular
							arcades
P14	Disorganization	No CME	Discontinuous Discontinuous	Discontinuous	Discontinuous	Discontinuous	Generalized hypo-AF with relatively
							preserved AF at posterior macula
P15	Disorganization	No CME	Discontinuous Discontinuous	Discontinuous	Discontinuous Discontinuous	Discontinuous	Generalized mottled hypo-AF
$P16^{a}$	1	1	1	1	1	1	
P17	Normal with coarse	No CME	Discontinuous Discontinuous	Discontinuous	Discontinuous Discontinuous	Discontinuous	Mottled hypo-AF at central macula
	lamination						
P18	Normal with coarse	No CME	Discontinuous Discontinuous	Discontinuous	Discontinuous Discontinuous	Discontinuous	Generalized hypo AF with hyper-AF
	lamination						spots around vascular arcades
P19	Normal with coarse	Parafoveal cyst OD at	Discontinuous Discontinuous	Discontinuous	Discontinuous	Discontinuous	Mottled hypo-AF with preservation of
	lamination	follow-up					AF between fovea and optic disc
P20	Normal organization	No CME	Continuous	Continuous	Continuous	Continuous	Mottled hypo-AF with preservation of
	and lamination						central macula
P21	Normal organization	No CME	Indiscernible	Indiscernible	Discontinuous	Discontinuous	Mottled hypo-AF changes at the
	and lamination						central macula with preservation
							outside the posterior pole
P22	Normal organization	No CME	Discontinuous Discontinuous	Discontinuous	Continuous	Continuous	Parafoveal hypo-AF with hyper-AF
	and lamination						foveal spot.

Clinical findings were similar between eyes, unless specifically mentioned. No qualitative changes were seen between baseline and 2-year follow-up in laminar organization, retinal band integrity and autofluorescence findings. AF = autofluorescence; CME = cystoid macular edema; ELM = external limiting membrane; EZ = ellipsoid zone; FAF = fundus autofluorescence; hypo-AF = hypo-autofluorescence; OD = right eye; ODS = right and left eyes; OS = left eye; SD-OCT = spectral domain optical coherence tomography. "OCT and FAF could not reliably be performed in this patient.

Inner retinal assessment Grade I: preserved retinal architecture With coarse lamination Grade III: disorganization of retinal structure with coarse lamination Grade III: disorganization of retinal structure with coarse lamination C C Outer retinal assessment Continuous ELM and EZ Indiscemible ELM and EZ

Supplemental Figure 1. Assessment of the inner retinal structure and the outer retinal band integrity using spectral-domain optical coherence tomography (SD-OCT). **A.** Grade I included patients with normal inner retinal structure and clear segmentation of individual layers. Note that the integrity of the outer retinal structures were not taken into consideration during grading. **B.** Patients with visible retinal delineation, but with a coarse aspect of individual layers were classified as grade II. **C.** Disorganization was defined as the inability to differentiate between adjacent inner retinal layers, which could be caused by the presence of cystoid macular edema. **D-F.** The external limiting membrane (ELM; white arrowhead) and ellipsoid zone (EZ; yellow arrowhead) were assessed at the peri- and parafovea. Retinal bands were classified as either continuous (relatively homogeneous reflectivity of the given band), discontinuous (heterogenous reflectivity and/or disruption of the given band) or indiscernible.